INSTITUT DE FRANCE
Académie des sciences

Comptes Rendus

Géoscience

Sciences de la Planète

Mohamed El Abd Bouha, Houssa Ouali, Muhammad Ouabid, Hicham El Messbahi and Abdelkader Mokhtari

Petrogenesis and crustal evolution of the Tasiast TTG suite (SW Reguibat Shield, Mauritania). Implication for crustal growth in the West African craton

Volume 353, issue 1 (2021), p. 19-35

Published online: 31 March 2021

https://doi.org/10.5802/crgeos.48

Les Comptes Rendus. Géoscience — Sciences de la Planète *sont membres du Centre Mersenne pour l'édition scientifique ouverte*
www.centre-mersenne.org
e-ISSN : 1778-7025

Comptes Rendus
Géoscience — Sciences de la Planète
2021, 353, nº 1, p. 19-35
https://doi.org/10.5802/crgeos.48

Review Article — Petrology, Geochemistry

Petrogenesis and crustal evolution of the Tasiast TTG suite (SW Reguibat Shield, Mauritania). Implication for crustal growth in the West African craton

Mohamed El Abd Bouha [a], Houssa Ouali [*, a], Muhammad Ouabid [b, c], Hicham El Messbahi [d] and Abdelkader Mokhtari [a]

[a] GEO3 Laboratory, Geology Department, Faculty of Sciences, Moulay Ismail University, P.O. Box 11201 Zitoune, Meknès, Morocco

[b] Geology & Sustainable Mining, Mohammed VI Polytechnic University, Plot 660, Hay Moulay Rachid, 43150, Benguerir, Morocco

[c] Instituto Andaluz de Ciencias de la Tierra (IACT), CSIC–UGR, Avenida de las Palmeras 4, 18100 Armilla, Granada, Spain

[d] Département de Géologie, Faculté Polydisciplinaire, Université Sidi Mohamed Ben Abdellah, Route d'Oujda, P.O. 20 Box 1223, Taza, Morocco

E-mails: moustafabouha@yahoo.fr (M. El Abd Bouha), houali@yahoo.fr (H. Ouali), muhaouabid@gmail.com (M. Ouabid), h.geo@hotmail.fr (H. El Messbahi), mokhtari57@yahoo.fr (A. Mokhtari)

Abstract. The Mauritanian Tasiast unit in the Southwestern Reguibat Archean Shield (North of the West African craton = WAC) consists mainly of gneiss dated between 3.07 and 2.91 Ga. We present new field and petrographic observations combined with whole-rock geochemical data on gneisses of Tasiast to understand their petrogenesis, tectonic setting, and the evolution of the continental crust of WAC. These data provide firm evidence of two distinct orthogneisses: trondhjemite and high-K granite affinities. Geochemical characters suggest that (1) trondhjemites magma source were originally derived from polybaric partial melting at the thickened crust occurred over a range of *P*–*T* conditions, covering the stability fields of garnet amphibolite and rutile eclogite. The trondhjemite composition is attributed to mixing of two major melts: one originating from eclogitic facies source region (high Nb/Ta) and the other from a garnet-amphibolite facies (low Nb/Ta) leaving garnet, amphibole, and rutile in the residue. (2) Compared to trondhjemite, the granites with high K_2O and Rb contents, and low Na_2O, Al_2O_3 and Sr contents suggest that basaltic oceanic crust was not their source material. Moreover, field relationships suggest that the granites were derived from partial melting of trondhjemites. Hence, the trondhjemite and high-K granites marked together two distinct stages during the growth of the continental crust in the Tasiast area.

Keywords. Trondhjemite, Granite, Amphibolite, Eclogite, Tasiast, Mauritania, West African craton.

Manuscript received 16th August 2020, revised 15th September 2020 and 29th January 2021, accepted 8th February 2021.

* Corresponding author.

1. Introduction

Tonalite–trondhjemite–granodiorite (TTG) suites constitute an important part of outcropped Archean rocks [e.g. Martin et al., 2005], and the studies of these silicic magmatism can provide significant information about the origin and chemical evolution of the primitive continental crust [e.g., Arndt, 2013, Barker and Arth, 1976, Condie, 2005, Dey et al., 2017, Drummond and Defant, 1990, Jahn et al., 1981, Martin et al., 2005, O'Neil and Carlson, 2017, Rudnick, 1995]. Mineralogically, TTGs are composed mainly of quartz + plagioclase and in lesser degrees, biotite and hornblende reflecting an evolved affinity with high content of SiO_2 (>68 wt%), Al_2O_3 (>15 wt%) and Na_2O (>3 wt%) and low K_2O/Na_2O (<0.5) ratios [e.g., Barker and Arth, 1976, Martin, 1994, Martin et al., 2005, Zhai and Santosh, 2011]. In addition, Archean TTGs are also characterized by steep negative rare-earth element (REE) patterns and low heavy REE abundances [Jahn et al., 1981, Martin, 1994, Martin et al., 2005]. Also, the trace element concentrations of typical TTGs exhibit enrichments in incompatible elements and negative Nb–Ta anomalies [e.g., Huang et al., 2013, Martin, 1994, 1999, Martin et al., 2005]. These Archean TTGs are generally interpreted to be the product of hydrous metabasalts partial melting [De Almeida et al., 2017, Foley, 2008, Foley et al., 2002, Martin, 1994, 1999, Martin et al., 2005, Moyen, 2009, Rapp and Watson, 1995, Rapp et al., 1999, 2003, Sen and Dunn, 1994, Winther and Newton, 1991]. However, it is difficult to distinguish between melting of garnet-bearing amphibolite and eclogite in terms of major and trace element chemistry [Foley, 2008, Foley et al., 2002, Hoffmann et al., 2014, Klemme et al., 2002, 2005, Martin, 1999, Rapp and Watson, 1995, Rapp et al., 1999, 2003, Xiong, 2006]. Furthermore, the geodynamic setting of TTG petrogenesis still remains controversial [e.g., Moyen et al., 2017 and references therein]. Consequently, three main models are proposed for the origin of TTGs and Archean crustal growth: TTGs can be formed by (1) partial melting of subducting oceanic crust. In this model, the hotter Archean mantle is responsible for melting (rather than dehydration) of metabasalts in subducted slabs; the Archean arc magmatism is therefore TTG in nature; (2) Partial melting of amphibolite/eclogite at the base of thickened arc crust. This model is probably the dominant petrogenetic model for the formation of the TTG suite [e.g., Moyen and Martin, 2012]; (3) Partial melting of wet mafic roots of an oceanic plateau [e.g. Van Kranendonk et al., 2007]. These last two models are primarily supported by the lack of clear arc-related features in the Archean geology [e.g., Hamilton, 1998, 2003], but it is difficult to admit a water supply at the base of the crust without evoking a subduction. In this paper, we present new field and petrographical observations, and whole-rock major and trace element data for the orthogneisses from the Tasiast Archean TTGs. The main purposes are (1) to provide new insights into the petrogenesis implications, (2) to assess the possible petrogenetic links between different orthogneisses, and (3) to understand the tectonic setting for the widespread Tasiast silicic magmatic units.

2. Geological setting

Reguibat Shield is the northernmost outcrop of the West African craton (Figure 1) [e.g., Ennih and Liégeois, 2008, Menchikoff, 1949]. It is surrounded on almost sides by Pan-African orogenic belts and covered in the south by the extensive intracratonic sediments of the Taoudeni Basin [e.g., Cahen et al., 1984, Ennih and Liégeois, 2008, Ouabid et al., 2017]. The major part of this craton is buried beneath various metamorphosed sediments, and unconsolidated superficial deposits of Sahara Atlantic coastal. Dillon and Sougy [1974] and Bessoles [1977] distinguished two provinces within the Reguibat Shield: (1) a Southwestern province composed of rocks with an age older than ca. 2 Ga (i.e., pre-Eburnean cycle); and (2) Central and North Eastern province consists of Eburnean rocks (Figure 1). The Reguibat Shield was cratonized at the end stage of the Eburnean orogeny (cs. 2.1–2 Ga) and has been stable since about 1.7 Ga [e.g., Schofield et al., 2006, Montero et al., 2014]. The Archean Shield contains grey gneiss, various acidic rocks, migmatites as well as mafic and ultramafic rocks (greenstone belt), quartzites and banded iron formations (BIF), and is characterized by regional foliations trajectories N–S to NE–SW in the southern part and NNW–SSE in its northern part [e.g., Chardon, 1997]. The southern part of the Shield is subdivided into three units which are from West to

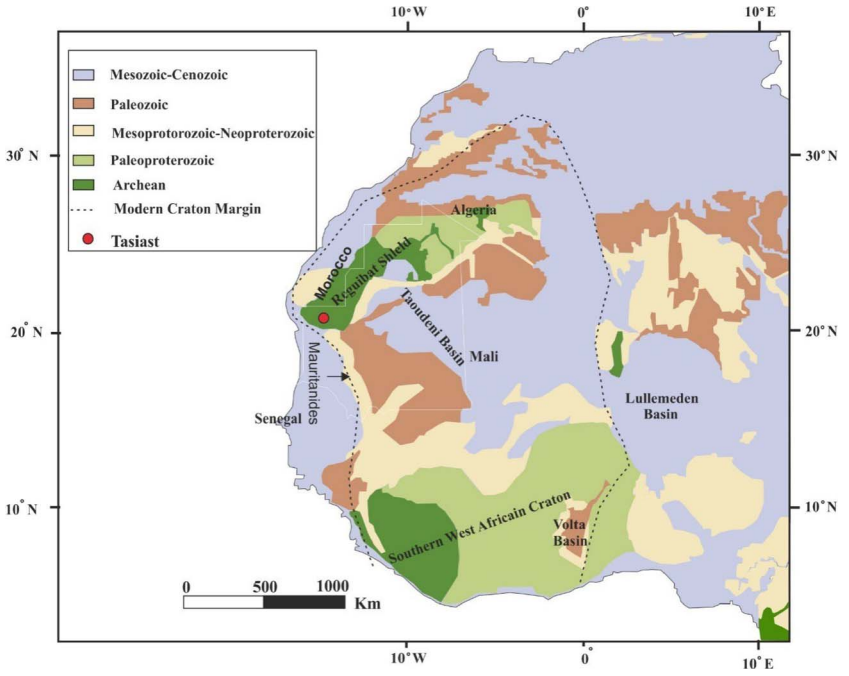

Figure 1. Geological framework of the West African craton showing the location of the studied Tasiast area in Mauritania [Chorlton, 2007].

East: Tasiast, Tijirit, and Amsaga; Tiris is the northernmost part. Tiris and Amsaga units have been affected by a regional granulite facies metamorphism, while Tasiast and Tijirit show greenschist or amphibolite metamorphic assemblages [Chardon, 1997]. The lithologies that make up the Tasiast terrains can therefore be divided into the following three major groups [e.g., Key et al., 2008]: (1) migmatitic gneisses with amphibolite lenses and minor orthogneisses; (2) greenstone belt lithologies; and (3) post-greenstone belt granitoids (mostly TTGs), granites, and minor pegmatitic muscovite granites that are the youngest intrusions.

The Tasiast–Tijirit terrane contains rocks with Nd model ages similar to Amsaga, between 3.6 Ga and 3.1 Ga, but zircon ages that only recorded magmatic events between 2.97 Ga and 2.89 Ga and a possible thermal imprint at ca. 2.7 Ga [Chardon, 1997, Key et al., 2008]. The Tiris terrane has the youngest Archean crust with Nd model ages between 3.2 Ga and 3.0 Ga, and zircon ages that reflect several magmatic events at 2.95 Ga, 2.65 Ga, and 2.48 Ga [Schofield et al., 2012]. An age U/Pb, between ca. 3.06 and 2.95 Ga obtained from inherited zircons xenocryst in three quartz veins along Tasiast thrust [Heron et al., 2016]; this age corresponds to previous ages obtained from the Tasiast–Tijirit terrane gneiss and TTG rocks. According to our field observations (Figure 1b–d), the Tasiast granitoid gneisses can be easily subdivided into grey and leucocratic suites (Figure 2b–d). The leucocratic suite appears clearly younger than grey gneiss. The field relationships between both units are clear; the leucocratic gneisses are either wrapping the grey gneisses unit or intruding them with a sharp contact. New petrographic observations of more than 30 samples from these gneiss units permit to distinguish between two types of granitoid facies: TTG gneiss and granitic gneiss.

3. Petrography

Grey gneisses occur as grey-dark rocks with coarse- to medium-grained texture (Figure 3a–e). They have a homogeneous minerals assemblage made of plagioclase (dominant: 45–60% vol. of the rock), quartz (25–35% vol.), biotite (5–15% vol.), and minor interstitial potassium feldspar (K-feldspar), and accessory minerals including magnetite, ilmenite, titanite, apatite,

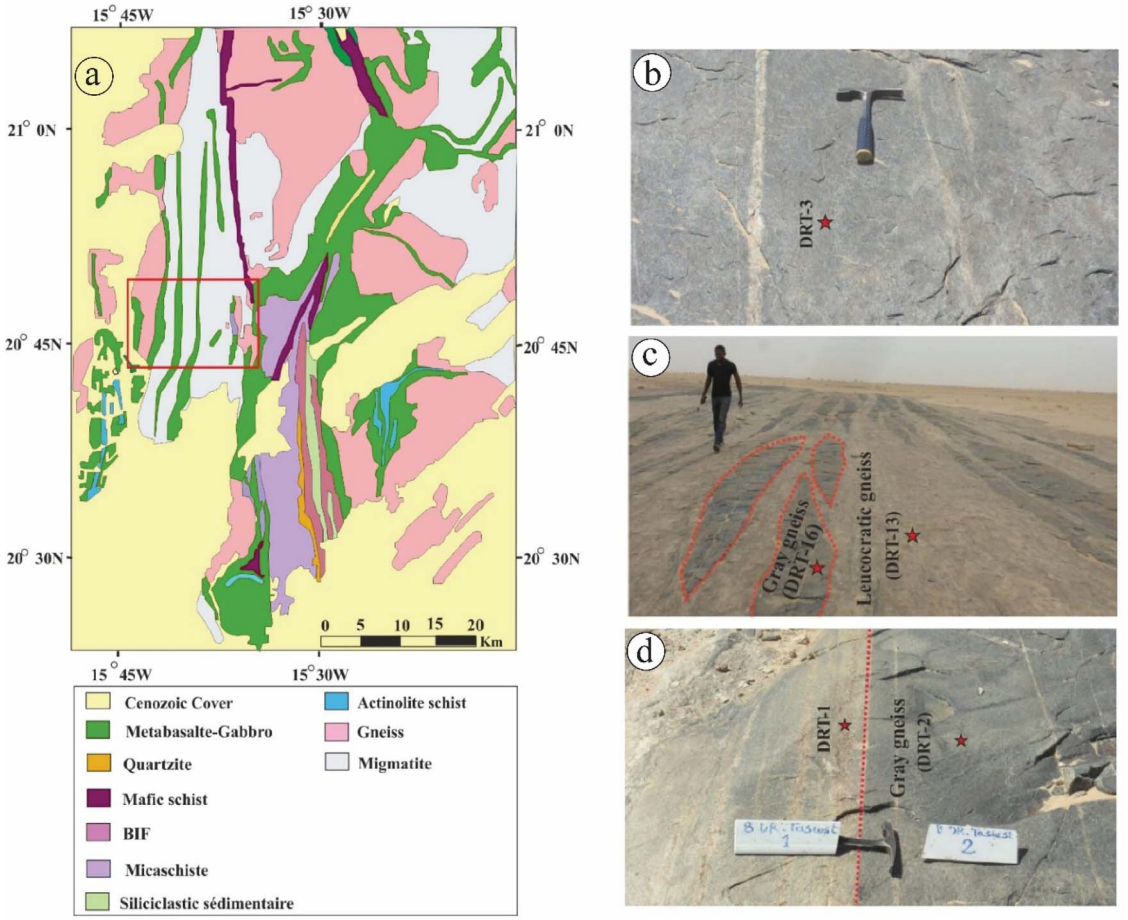

Figure 2. (a) Geological map of the Tasiast area [adapted from PRISM 1:500k geological map; in Heron et al., 2016]. (b–d) Field photographs illustrating lithological aspects and field relationships in the Tasiast area.

and zircon. Generally, the grey gneiss occurs with two alternating layers: quartz and plagioclase-rich layer (clear) and biotite-rich layer (dark), which give the rock its gneissic foliation. Plagioclase crystals are euhedral to subhedral (1–4 mm in size) mostly altered to albite and sericite and enclose frequently biotite and apatite. Quartz ranges from interstitial to fine aggregates (0.1–0.5 mm in size), surrounding the large plagioclase crystals. Biotite occurs strongly as pleochroic flakes which are partially altered to chlorite, titanite, and opaque minerals, or exhibits elongated crystal around plagioclase or enclosed in this mineral. K-feldspar (mainly microcline) is interstitial between quartz and plagioclase grains.

Leucocratic gneisses are a medium-grained and yellow pale leucocratic rock with gneissic texture as well as the previous rock (Figure 3g–i). Major mineral phases are quartz (40–45% vol.), K-feldspar (35–40% vol.), plagioclase (10–15% vol.) and biotite (<4% vol.). Like the previous facies, titanite, Fe–Ti oxides (magnetite and ilmenite), apatite, and zircon are common accessory minerals in these granitic rocks. Quartz occurs as polycrystalline aggregates (0.2–2 mm in size) developed around primary crystals of feldspars or as fabric of alternated quartz and feldspar-rich layers. K-feldspar (principally orthoclase) and plagioclase occurs mainly as subhedral phenocrysts (1–3 mm in size) wrapped by the fine- to medium-grained matrix composed of K-feldspar and quartz aggregates. Biotite is scarce and occurs as elongated crystals with

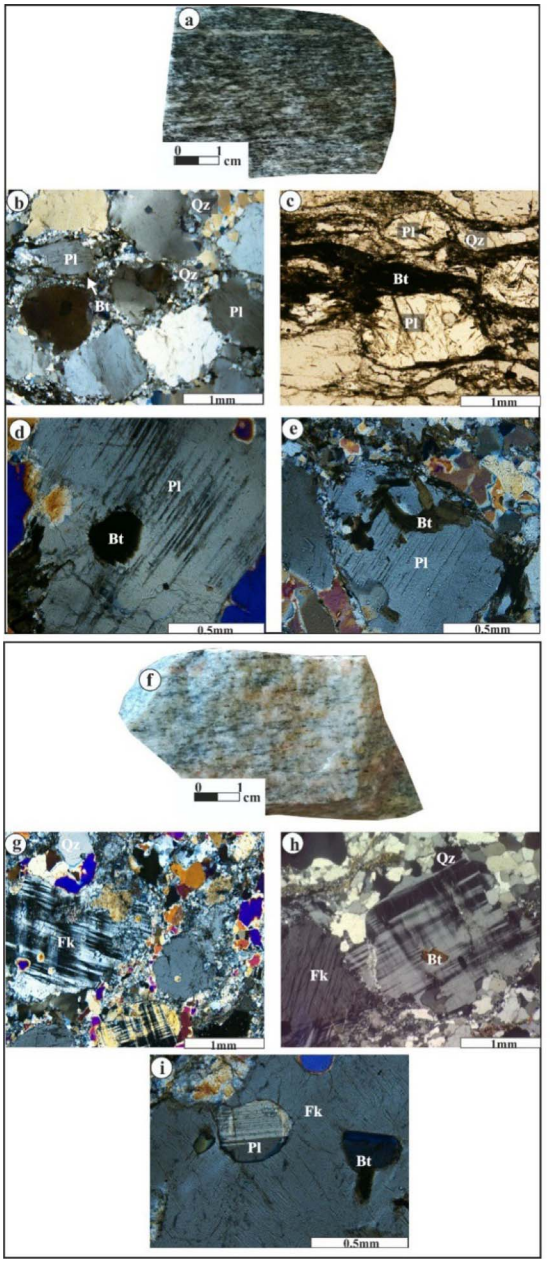

Figure 3. Hand specimens and microscope photographs of the Tasiast gneiss types. (a–e) Grey gneisses. (f–i) Leucocratic gneisses.

preferential orientation parallel to the feldspar and quartz layers.

4. Analytical methods

Sixteen representative samples of the two distinct granitoid gneisses of the Tasiast unit were selected for whole-rock geochemical analyses, including eleven Grey gneiss and five leucocratic gneisses (compositions are given in Table 1). Rocks were analysed at the Instituto Andaluz de Ciencias de la Tierra (IACT, Granada, Spain). Rock powders were prepared using a jaw crusher and an agate ring mill. Whole-rock analyses of major elements and V, Cr, Co, Zr, and Ni were determined by X-ray fluorescence (XRF). Loss on ignition (LOI) was determined by drying the samples at 900 °C and is low (0.12–0.46 wt%). Trace elements (except V, Cr, Co, Zr, and Ni) were analysed using a Triple Quadrupole Agilent 8800 inductively coupled plasma mass spectrometer (ICP-MS) at the IACT laboratory. Sample digestion was performed following the HF–$HClO_4$ digestion process described by Garrido et al. [2000]. Element concentrations were determined by external calibration, except for Hf that was calculated using Zr measured by XRF and the chondritic Zr/Hf ratio [McDonough and Sun, 1995]. The compositions of the granite reference sample GS-N, analysed as unknown during the analytical runs, show good agreement with published values of this international standard [Georem database; Jochum et al., 2016].

5. Whole-rock geochemistry

In the anorthite (An)–orthoclase (Or)–albite (Ab) [Barker, 1979, O'Connor, 1965] and quartz (Qz)–Or–Ab [Barker and Arth, 1976] CIPW normative diagrams, the eleven analyzed samples of grey gneiss from Tasiast region are plotted in the field of trondhjemite series while the five samples of leucocratic gneisses are classified as granites (Figure 4), which consistent with field and petrographic conclusions.

The trondhjemitic gneisses have SiO_2 contents ranging from 69.92 to 72.72 wt% and high Al_2O_3 contents (15.14–16.22 wt%) (Table 1). They have relatively low MgO [0.39–0.83 wt%, Mg# = Mg/(Mg + Fe) : 0.37–0.47]. Trondhjemite samples have slight enrichment in Na_2O (4.73–5.46 wt%) and CaO (1,81–2.92 wt%) with low K_2O contents (1.15–2.80; K_2O/Na_2O ~ 0.21–0.58) and classified mostly as calc-alkaline series as shown in the diagram of Peccerillo and Taylor [1976] (Figure 5). The compositions of all the investigated trondhjemite rocks generally overlap those of

Table 1. Major (wt%) and trace (ppm) element concentrations for the grey gneisses in the Tasiast area

Sample N	DRT2	DRT3	DRT4	DRT5-1	DRT6	DRT7	DRT9	DRT11	DRT14	DRT15	DRT16
SiO_2	70.92	72.72	71.98	70.11	70.69	69.92	70.62	71.91	70.38	70.68	70.19
TiO_2	0.30	0.19	0.20	0.30	0.29	0.34	0.29	0.20	0.30	0.29	0.30
Al_2O_3	15.99	15.21	15.16	16.10	15.88	16.04	15.92	15.14	16.01	16.16	16.22
Fe_2O_3	1.80	1.32	1.20	2.02	1.70	2.13	1.85	1.28	1.81	1.85	1.96
MnO	0.04	0.03	0.01	0.05	0.03	0.04	0.04	0.03	0.03	0.03	0.04
MgO	0.77	0.39	0.42	0.80	0.69	0.81	0.70	0.41	0.74	0.83	0.76
CaO	2.55	1.81	1.84	2.67	2.66	2.92	2.65	1.95	2.78	2.83	2.69
Na_2O	5.14	4.97	4. 73	5.46	5.08	5.06	5.20	4. 81	5.13	4.96	5.37
K_2O	1.60	2.52	2.73	1.15	1.60	1.32	1.44	2.80	1.44	1.71	1.36
P_2O_5	0.13	0.06	0.08	0.12	0.11	0.13	0.11	0.06	0.12	0.16	0.12
LOI	0.37	0.23	0.40	0.37	0.20	0.18	0.16	0.46	0.27	0.37	0.24
Total	99.25	99.21	98.34	98.78	99.01	98.71	98.82	98.59	98.72	99.50	99.01
Mg#	46	37	41	44	45	43	43	39	45	47	43
Cs	1.11	0.49	0.52	1.63	1.38	1.23	1.72	0.55	4.27	1.57	1.40
Zr	116	130	143	132	126	137	129	134	125	128	130
Hf*	3.13	3.51	3.86	3.56	3.40	3.70	3.48	3.62	3.38	3.46	3.51
Cr	—	—	—	—	—	—	—	—	—	—	—
Ni	—	—	—	—	—	—	—	—	—	—	—
Rb	32.42	69.84	67.71	30.36	41.17	37.96	39.48	91.55	67.26	58.15	56.46
Sr	342.05	402.39	372.82	304.08	477.68	473.78	377.75	438.87	385.54	516.70	313.63
Y	2.73	1.12	1.37	3.18	1.94	2.66	2.33	2.08	2.56	2.22	3.15
Nb	3.52	2.30	2.69	3.78	2.16	2.33	3.06	3.33	4.04	3.17	4.63
Ba	678.26	1268.04	1485.09	139.42	637.09	630.18	435.23	1264.02	458.45	878.33	226.05
La	12.12	33.39	26.95	16.87	17.73	15.72	16.63	16.95	19.37	17.68	19.40
Ce	22.98	53.80	43.31	30.63	31.68	31.01	30.20	27.02	35.79	34.83	35.32
Pr	2.40	4.48	3.94	3.03	3.17	3.05	3.04	2.37	3.37	3.27	3.50
Nd	9.03	14.15	12.14	10.92	11.41	11.36	11.29	7.62	12.11	11.92	12.42
Sm	1.33	1.73	1.58	1.52	1.66	1.74	1.57	1.12	1.66	1.53	1.69
Eu	0.55	0.47	0.55	0.38	0.55	0.63	0.42	0.50	0.44	0.62	0.37
Gd	0.99	0.94	0.95	1.12	1.03	1.15	0.97	0.79	1.03	1.00	1.21
Tb	0.12	0.11	0.10	0.14	0.12	0.14	0.13	0.10	0.14	0.11	0.16
Dy	0.56	0.33	0.37	0.66	0.45	0.62	0.49	0.47	0.56	0.43	0.71
Ho	0.10	0.04	0.05	0.11	0.08	0.09	0.08	0.07	0.09	0.07	0.11
Er	0.23	0.08	0.10	0.28	0.16	0.22	0.21	0.21	0.24	0.21	0.32
Tm	0.03	0.01	0.01	0.04	0.02	0.03	0.03	0.03	0.03	0.03	0.03
Yb	0.22	0.07	0.08	0.22	0.13	0.19	0.14	0.14	0.16	0.19	0.19
Lu	0.03	0.01	0.01	0.03	0.02	0.03	0.02	0.02	—	0.03	0.03
Ta	0.21	0.08	0.09	0.16	0.14	0.15	0.15	0.17	0.36	0.17	0.28
Pb	6.85	16.99	16.31	6.18	7.77	6.54	8.73	21.20	8.93	10.49	10.84
U	0.76	0.96	0.71	0.78	0.88	1.24	0.59	1.97	1.15	2.97	2.88
A/NK	1.57	1.39	1.41	1.57	1.57	1.64	1.57	1.38	1.60	1.61	1.57
A/CNK	1.08	1.07	1.08	1.07	1.06	1.06	1.07	1.04	1.06	1.06	1.07
K_2O/Na_2O	0.31	0.51	0.58	0.21	0.31	0.26	0.28	0.58	0.28	0.35	0.25
FMMT	2.73	1.79	1.70	2.97	2.53	3.10	2.69	1.79	2.69	2.81	2.86
Sr/Y	125.47	359.85	271.97	95.73	245.73	178.08	162.19	210.83	150.36	232.55	99.55
(La/Yb)N	38.25	333.28	233.89	52.43	92.69	56.84	81.22	83.49	83.48	63.99	71.35
Nb/Ta	16.65	30.23	29.13	24.01	14.98	15.62	20.23	19.51	11.26	18.88	16.33
Zr/Sm	87.19	75.26	90.40	86.69	75.73	78.76	82.04	120.17	75.08	83.52	76.74
Dy/Yb	2.53	4.75	4.59	2.97	3.42	3.26	3.43	3.34	3.51	2.26	3.76

(continued on next page)

Table 1. (continued)

Sample N	DRT2	DRT3	DRT4	DRT5-1	DRT6	DRT7	DRT9	DRT11	DRT14	DRT15	DRT16
Eu/Eu*	1.39	1.01	1.26	0.85	1.19	1.28	0.96	1.55	0.95	1.42	0.75
Nb/Nb*	0.24	0.14	0.21	0.26	0.13	0.10	0.27	0.10	0.18	0.06	0.09
Pb/Pb*	3.42	3.95	4.56	2.37	2.86	2.48	3.37	9.63	2.98	3.61	3.60
Sr/Sr*	2.11	1.43	1.52	1.51	2.27	2.31	1.85	2.93	1.73	2.37	1.36
Ti/Ti*	0.56	0.40	0.38	0.66	0.54	0.55	0.65	0.43	0.64	0.50	0.65
Ta/Ta*	0.46	0.07	0.10	0.26	0.24	0.28	0.26	0.28	0.52	0.27	0.40
∑RRE	50.86	109.61	90.14	65.97	68.23	65.97	65.23	57.41	74.98	71.92	75.46
Nord	20.7909°	20.7910°	20.7900°	20.7961°	20.7986°	20.7984°	20.7960°	20.7947°	20.7935°	20.7943°	20.7936°
West	15.7052°	15.6817°	15.6810°	15.6817°	15.6813°	15.6810°	15.6767°	15.6967°	15.6894°	15.7088°	15.709°

Hf had been calculated after Zr concentration. A/CNK = molar ratio of $Al_2O_3/(CaO + Na_2O + K_2O)$; A/NK = molar ratio of $Al_2O_3/(Na_2O+K_2O)$; Mg# = molar ratio of $(MgO/40.3)/((MgO/40.3)+(FeO/71.85)) * 100$; (La/Yb)cn are chondrite-normalized values [from Sun and McDonough, 1989].

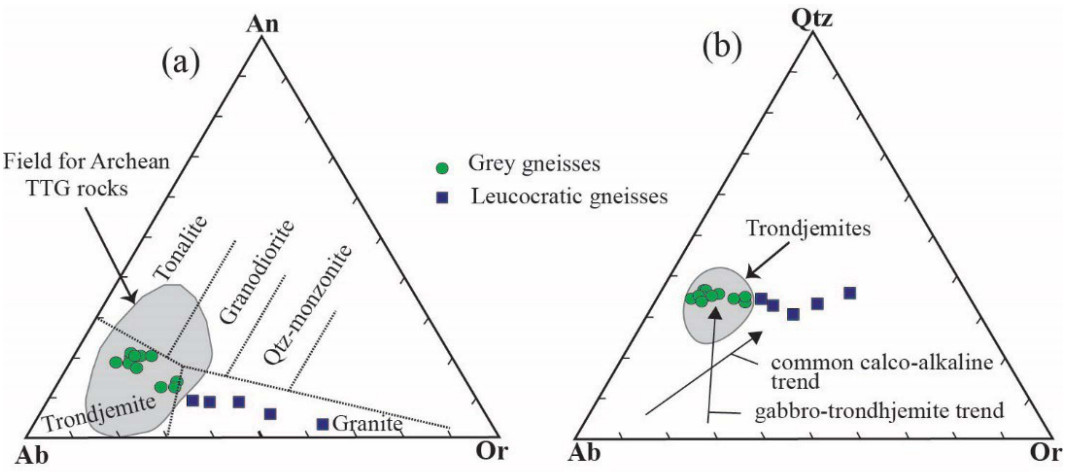

Figure 4. Classification of Tasiast gneisses using normative An–Ab–Or [Barker, 1979] and Qz–Or–Ab [Barker and Arth, 1976].

the Archean TTGs as shown in Figure 4(a, b) [TTG field from Smithies and Champion, 1998 and Barker and Arth, 1976].

On the other hand, according to the petrographic observations and in contrast to previous gneiss, the granitic gneisses are silica rich with SiO_2 contents ranging between 71.99 wt% and 74.54 wt% and they are characterized by moderate Al_2O_3 concentrations (13.39–15.08 wt%). Moreover, they are classified as high-K calc-alkaline to shoshonitic series with high K_2O (3.25–6.28 wt%), moderate Na_2O (2.71–4.69 wt%), and low CaO (0.64–1.43 wt%) concentrations (Figure 5; Table 2). Furthermore, all the investigated samples of trondhjemite and granite gneisses are peraluminous [mol. $Al_2O_3/CaO + Na_2O + K_2O$ = A/CNK > 1 and mol. $Al_2O_3/Na_2O + K_2O$ = A/NK > 1; Maniar and Piccoli, 1989; Figure 6; Tables 1 and 2]. In contrast to the trondhjemite samples, the compositions of the studied leucocratic gneisses contrast starkly with Archean TTGs, and show a common trend for calc-alkaline granites (Figure 4a, b).

The primitive mantle-normalized trace element spider and chondrite-normalized REE patterns are shown in Figure 7. The Tasiast trondhjemitic gneisses are enriched on high field strength elements (HFSE) such as Rb, Ba, U, Pb, and Sr (Sr/Sr^* ~ 1.36–2.93) and strongly depleted in Nb (Nb/Nb^* ~ 0.06–0.27), Ta (Ta/Ta^* ~ 0.07–0.52), and Ti (Ti/Ti^* ~ 0.38–0.66) with high Sr/Y (95.7–359.8). They have highly variable Nb/Ta (11.26–30.23) ratios. On the chondrite-normalized REE diagrams, trondhjemites show similar moderate REE concentrations (ΣREE ~ 50.86–

Table 2. Major (wt%) and trace (ppm) element concentrations for the leucocratic gneisses in the Tasiast area

Sample N	DRT1	DRT5-2	DRT8	DRT12	DRT13
SiO_2	73.59	73.83	71.99	74.54	73.49
TiO_2	0.09	0.06	0.09	0.08	0.07
Al_2O_3	14.66	14.26	15.08	13.39	14.60
Fe_2O_3	0.89	0.37	0.97	1.40	0.68
MnO	0.02	0.01	0.03	0.03	0.03
MgO	0.24	—	0.21	—	—
CaO	1.33	1.00	1.43	0.64	1.41
Na_2O	4.47	3.56	4. 05	2.71	4.69
K_2O	3.83	5.56	4.57	6.28	3.25
P_2O_5	0.03	0.04	0.03	0.06	0.04
LOI	0.23	0.33	0.23	0.12	0.12
Total	99.14	98.69	98.44	99.14	98.26
Mg#	35	—	30	—	—
Cs	0.39	0.76	0.81	0.64	0.59
Zr	80	43	85	16	57
Hf	2.16	1.16	2.30	0.43	1.54
Cr	—	—	—	2.00	—
Ni	—	—	—	—	—
Rb	77.96	169.18	112.84	183.48	82.50
Sr	110.94	145.14	357.85	264.50	180.57
Y	1.48	1.95	1.40	0.53	1.34
Nb	3.70	1.58	1.73	1.35	2.90
Ba	682.22	624.73	1451.56	1960.53	1197.09
La	7.66	13.70	21.37	6.25	8.36
Ce	12.32	25.16	40.09	10.99	14.66
Pr	1.26	2.51	3.58	0.98	1.31
Nd	4.26	8.73	12.17	3.30	4.77
Sm	0.83	1.65	1.80	0.49	0.94
Eu	0.24	0.30	0.54	0.52	0.36
Gd	0.56	1.15	1.09	0.31	0.60
Tb	0.08	0.13	0.11	0.04	0.08
Dy	0.34	0.54	0.41	0.15	0.37
Ho	0.05	0.07	0.05	0.02	0.05
Er	0.12	0.15	—	0.04	0.11
Tm	0.02	0.02	0.01	—	0.01
Yb	0.10	0.10	0.08	0.03	0.10
Lu	0.02	0.01	0.02	—	0.02
Ta	0.12	0.13	0.12	0.10	0.07
Pb	12.75	22.45	23.95	24.03	18.25

(continued on next page)

Table 2. (continued)

Sample N	DRT1	DRT5-2	DRT8	DRT12	DRT13
U	1.78	11.93	0.89	1.14	1.45
A/NK	1.30	1.30	1.27	1.19	1.20
A/CNK	1.06	1.04	1.05	1.08	1.06
K_2O/Na_2O	0.86	1.56	1.13	2.32	0.69
FMMT	1.15	0.40	1.20	1.37	0.71
Sr/Y	74.80	74.49	255.33	500.02	135.17
(La/Yb)N	51.15	91.29	178.40	146.12	59.11
Nb/Ta	31.83	12.61	14.27	13.30	38.67
Zr/Sm	96.96	26.02	47.27	32.67	60.76
Dy/Yb	3.26	5.22	4.93	4.94	3.80
Eu/Eu*	0.99	0.62	1.08	3.83	1.38
Nb/Nb*	0.12	0.01	0.11	0.07	0.11
Pb/Pb*	11.99	10.43	7.28	26.71	15.18
Sr/Sr*	1.37	0.89	1.54	4.20	2.07
Ti/Ti*	0.35	0.15	0.16	0.20	0.20
Ta/Ta*	0.35	0.28	0.18	0.45	0.23
∑REE	27.85	54.23	81.33	23.11	31.73
Nord	20.7909°	20.7961°	20.7950°	20.7938°	20.7933°
West	15.7052°	15.6817°	15.6765°	15.6895°	15.6897°

Hf had been calculated after Zr concentration. A/CNK = molar ratio of $Al_2O_3/(CaO + Na_2O + K_2O)$; A/NK = molar ratio of $Al_2O_3/(Na_2O + K_2O)$; Mg# = molar ratio of (MgO/40.3)/((MgO/40.3) + (FeO/71.85)) ∗100; (La/Yb)cn are chondrite-normalized values [from Sun and McDonough, 1989].

109.61 ppm) with high fractionations between LREE and HREE [$(La/Yb)_{cn}$ ~ 38.25–333.28], high fractionations between the HREE [$(Gd/Yb)_{cn}$: 3.72–6.40)], and negligible to positive Eu anomalies (Eu/Eu* ~ 0.75–1.55). On the other hand, the granitic gneisses are characterized by low REE concentrations (ΣREE ~ 23.11–81.33 ppm), significant variations in REE patterns in terms of fractionation [$(La/Yb)_{cn}$ ~ 51.15–178.40; [$(Gd/Yb)_{cn}$ ~ 4.50–10. 89)], and Eu anomaly (Eu/Eu* ~ 0.62–3.83). Spider diagrams show an enrichment of HFSE (e.g., Rb, Ba, U, and Pb), positive Sr anomaly (Sr/Sr* up to 4.20), and a strong negative anomaly of Nb (Nb/Nb* ~ 0.01–0.12), Ta (Ta/Ta* ~ 0.18–0.45), and Ti (Ti/Ti* ~ 0.15–0.35). All samples have high Sr/Y ratio (~74–500).

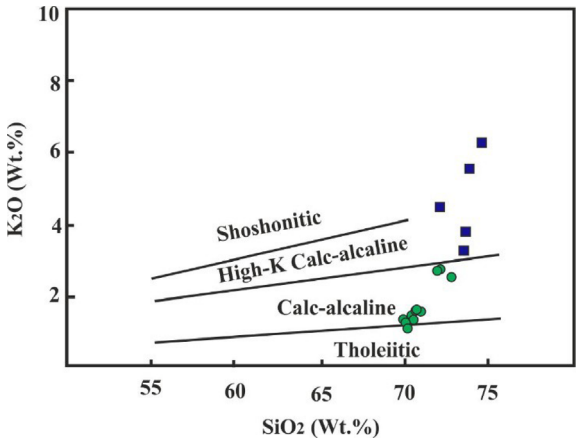

Figure 5. K_2O versus SiO_2 [Peccerillo and Taylor, 1976] (symbols are as in Figure 4).

6. Discussion

6.1. *Petrogenesis of trondhjemitic gneisses*

Generally, the TTG suites (trondhjemite, tonalite, and granodiorite) represent the major component of the Archean juvenile continental crust [Jahn et al., 1981, Laurent et al., 2014, Smithies et al., 2019]. Our new field and petrographic observations, and geochemical investigations confirm the widespread of trondhjemite in the Mauritanian Tasiast Archean unit. This unit is previously dated at about 3.07–2.91 Ga [Chardon, 1997, Heron et al., 2016, Key et al., 2008; Figures 2, 7]. The Tasiast trondhjemitic studied samples have typical Archean TTGs signatures (Figure 4a, b). In detail, these rocks are silica and alumina rich ($SiO_2 > 68$ wt%; $Al_2O_3 \geq 15$ wt%) and have low FMMT contents ($Fe_2O_3^{tot} + MgO + MnO + TiO_2 < 5$ wt%) [e.g., Martin, 1994]. The high Na_2O and low K_2O (Figure 5 and Table 1), resulting in a strong enrichment in plagioclase and absence of alkali feldspar as shown petrographic observations, suggest a derived mafic source rather than felsic one for these granitoids [e.g., Moyen, 2009]. The low Rb/Sr ratio and pronounced negative Nb, Ta, and Ti anomalies, and a strong fractionated displaying similar degrees of fractionation for both LREE and HREE, show that Tasiast trondhjemites are similar to most TTG [e.g., Condie, 1989, 1993, Jahn, 1994, Martin, 1994, Martin et al., 2005, Tarney et al., 1982]. In addition, high A/NK (1.38–1.61), A/CNK (1.04–1.08), Sr/Y (95.73–359.85), and $(La/Yb)_{cn}$ (38.25–333.25) ratios characterize high-Al TTGs and adakites [Figure 8(a, b); e.g., Martin, 1999, Martin et al., 2005].

In terms of acidic magma origin, many experimental and geochemical studies concluded that most TTGs are derived from a hydrated crust, although physical conditions are still debated [e.g., Foley et al., 2002, Hoffmann et al., 2011, Rapp et al., 2003]. The TTG melting occurred over a range of P–T conditions, covering the stability fields of garnet amphibolite and rutile eclogite. There are two common tectonic scenarios to produce TTG magmas: (1) melting of subducted oceanic crust; and (2) melting at the base of a mafic crust [e.g., Condie, 2005, Drummond and Defant, 1990, Hoffmann et al., 2011, 2014, Martin and Moyen, 2002, Martin et al., 2005, 2014, Moyen, 2011, Moyen and Martin, 2012, Smithies, 2000]. Subduction-related TTG magmas tend to possess high Mg#, Cr, and Ni contents due to interactions between the TTG melts and the mantle wedge [e.g., Martin and Moyen, 2002, Martin et al., 2005, Moyen and Martin, 2012, Smithies, 2000]. Anyway, the studied Tasiast TTG units have low MgO concentration (0.39–0.83 wt%, Mg# = 37–47) indicating an absence of interaction of studied TTG magmas with peridotite in the mantle wedge [e.g., Condie, 2005, Martin et al., 2005, Rapp et al., 1999, Smithies, 2000]. Therefore, it is more likely that the Tasiast trondhjemites were generated at the base of a thick mafic crust. The resulted melt involving basalts or amphibolites under various P_{H_2O} conditions below 10 Kbar were tonalitic in composition, without any trondhjemitic affinity; the garnet is not stable in these conditions [e.g., Beard and Lofgren, 1989, 1991, Helz, 1976, Holloway and Burnham, 1972, Rushmer, 1991]. According to field and petrographic observations, and geochemistry data, there are no tonalitic rocks among Tasiast gneiss units [Figures 2–4; e.g, Key et al., 2008]. Also, we notice that the majority of studied Tasiast TTG samples have a positive or no Eu anomalies accompanied by pronounced Sr anomalies (Figure 7a, b) that could reflect melting at pressures above the plagioclase stability field. Furthermore, the high Sr abundances (304–516 ppm) and low Y (<3.18 ppm) generating the high Sr/Y ratios in the trondhjemite rocks of Tasiast region (Figure 8a), indicating that the plagioclase was not in the residue and the depth of melting is above plagioclase stability field [e.g., Martin et al., 2005]. In addition, the Tasiast trondhjemitic gneisses display a pronounced enriched LREE relative to HREE patterns with high $(La/Yb)_{cn}$ and low Yb_{cn} (Figures 7b, 8b, Table 1), which are consistent with garnet in the residue [e.g., Martin et al., 2005].

Moreover, melts with pure amphibole in the residue would have low Nb/Ta, Gd/Yb, and Dy/Yb ratios, and high Zr/Sm ratios [e.g., Foley et al., 2002, Rapp et al., 2003, Zhou et al., 2014]; while the amphibole and garnet as a residual phases will not only effectively raise the Sr/Y, La/Yb, and Zr/Sm ratios with variable Nb/Ta ratio, but also increase the Gd/Yb and Dy/Yb ratios in the produced melts [e.g., Davidson et al., 2007, Macpherson et al., 2006]. The Tasiast trondhjemites have variable Nb/Ta (11.26–30.23), high Gd/Yb (4.5–1.4), Dy/Yb (2.3–4.7), and Zr/Sm (>75) indicating that the TTG gneisses were derived by partial melting of a source with garnet and amphibole in the residue. These characteristics make the trondhjemite rocks of Tasiast unit different from the

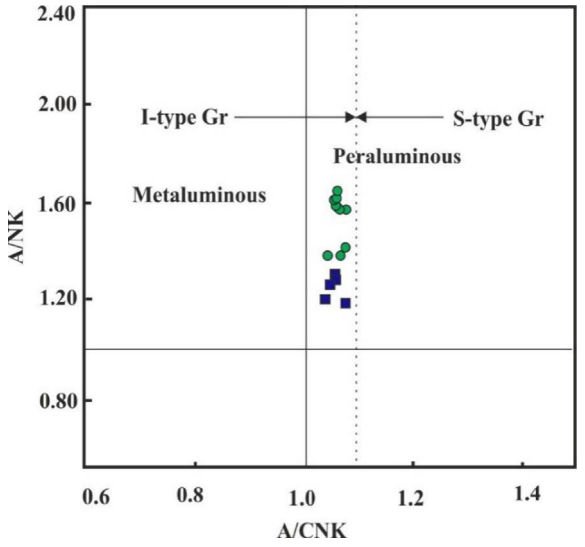

Figure 6. Investigated Tasiast granitoid gneisses in A/NK versus A/CNK diagram [Maniar and Piccoli, 1989] (symbols are as in Figure 4).

low-pressure TTGs described by Moyen and Martin [2012].

In the primitive mantle-normalized trace element diagram (Figure 7a), the trondhjemites are strongly depleted in Nb and Ta, which are consistent with rutile or/and amphibole in the residue [e.g., Martin et al., 2005, Zhou et al., 2014]. Consequently, these mineral phases involve in controlling the HFSE ratios such as Nb/Ta, Zr/Hf, and Zr/Sm because these elements pairs have different partition coefficients in different residual mineral phases [e.g., Foley et al., 2002, Jenner et al., 1994, Klemme et al., 2002, Rubatto and Hermann, 2003, Xiong et al., 2007]. So these ratios can be used as powerful evidence to discriminate between different source regions [e.g., Hoffmann et al., 2011]. Rutile and amphibole are two diagnostic minerals in eclogite facies and amphibolite facies conditions, respectively [Foley et al., 2002, Rapp et al., 2003]. Therefore, the Nb/Ta and Zr/Sm ratios can be used to recognize the conditions of melting: eclogite facies or amphibolite facies [Hoffmann et al., 2011]. Foley et al. [2002] investigated the distribution of HFSE in TTG liquids and concluded that the low Nb/Ta and high Zr/Sm ratios in Archean TTG preclude an eclogitic residue but are consistent with a garnet-bearing amphibolite. Both residues cannot explain the compositional trends found for trondhjemites of Tasiast. The variable Nb/Ta (11.26–30.23) and high Zr/Sm (75.08–120.17) ratios clearly in favour of polybaric melting occurred over a range of *P*–*T* conditions, covering the stability fields of garnet amphibolite and rutile eclogite as illustrated in Figure 9. Therefore, we attribute the TTG compositions to mixing of two major melts: the first is originating from eclogitic facies source regions (high Nb/Ta) and the second is formed from a garnet-amphibolite source (low Nb/Ta).

6.2. *Petrogenesis of granitic gneisses*

Compositional differences between granitic and trondhjemitic gneisses in the Tasiast area are remarkable. In contrast to the trondhjemite, the granites have high K_2O and Rb, and low Na_2O, Al_2O_3 and Sr contents (see Figures 5–7 and Table 2). Unlike TTGs ($K_2O < 2.84$), a high K_2O ($K_2O \sim 3.3$–6.34) content in granites suggest that basaltic oceanic crust was not their source material [e.g., Smithies, 2000]. According to Patino Douce [2005], the partial melting of anhydrous TTG within the middle or lower crust could produce granitic melts. The depleted HREE, Y and high La_{cn}/Yb_{cn} (~51–178) exhibited by studied Tasiast granite samples indicate the role of high fractions of residual garnet in their sources or an HREE-depleted source similar to that produced by the trondhjemites (Figures 7, 8, Table 2). In addition, the contribution of Watkins et al. [2007] highlighted that the melting of TTGs with low K_2O/Na_2O (<0.3) could not generate high-K granites. As the Tasiast trondhjemites have an average value of K_2O/Na_2O at about 0.36 (0.21–0.58), these trondhjemites seem to be the main suitable source of the granites studied here. Furthermore, the field relations between the trondhjemite and the granite clearly support this hypothesis (Figure 2).

6.3. *Continental evolution in the Tasiast Archean unit*

Archean TTGs show secular variation in composition indicating change in geodynamic setting of their formation or cooling of the Earth [e.g., Martin and Moyen, 2002, Smithies, 2000]. The geochemistry data of the Tasiast trondhjemite suggest that the most reasonable mechanism for the origin of these rocks is

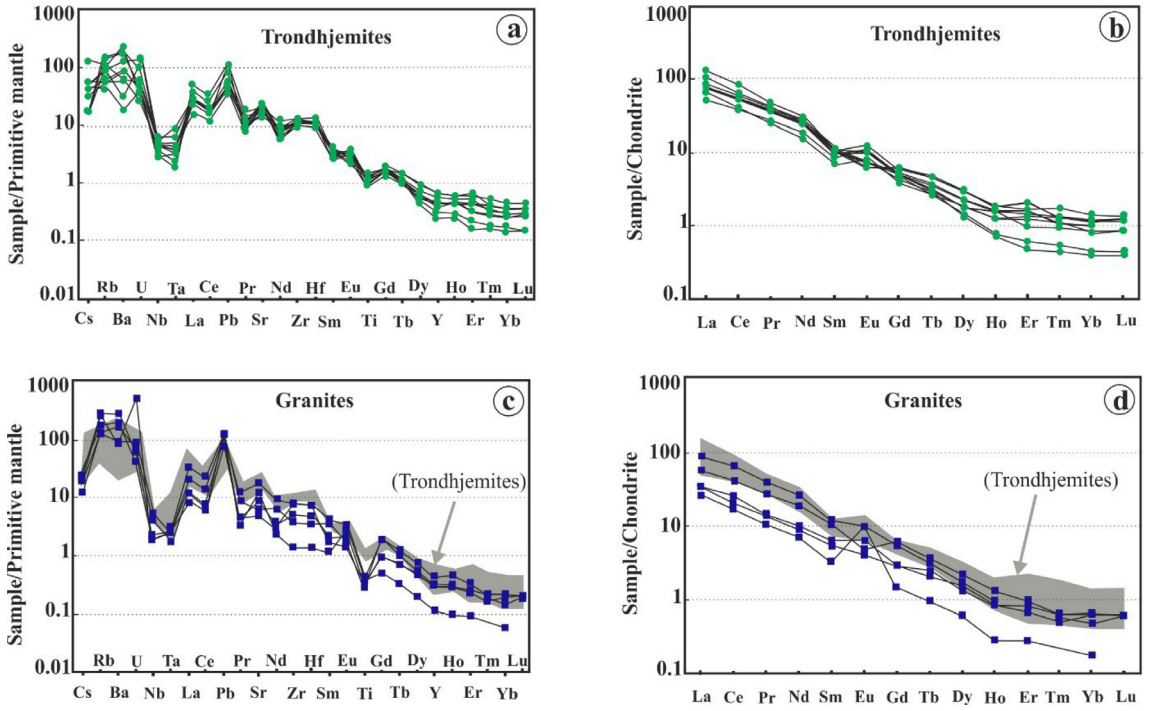

Figure 7. Primitive mantle-normalized trace elements patterns (a, c) and chondrite-normalized REE (b, d) of the trondhjemites, and granites in the Tasiast area [Sun and McDonough, 1989], (symbols are as in Figure 4).

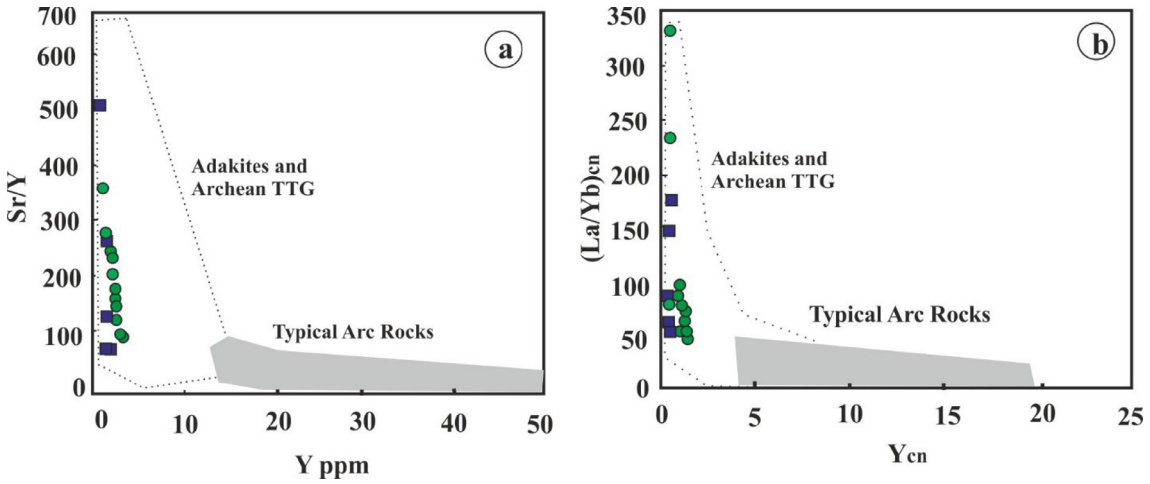

Figure 8. Sr/Y–Y adapted from Martin et al. [2005] (a) and La/Ybcn–Ybcn diagrams adapted from Martin [1999] (b) for Tasiast trondhjemites and granites. (Symbols are as in Figure 4).

the partial melting at the base of a thickened mafic crust covering the stability fields of garnet amphibolite and rutile eclogite (see Section 6.1). On the other hand, the trace element variations of granitic rocks were probably controlled mainly by source compositions and melting conditions rather than tectonic settings [e.g., Wu et al., 2003]. Their geochemical characteristics are likely inherited from the trondhjemite

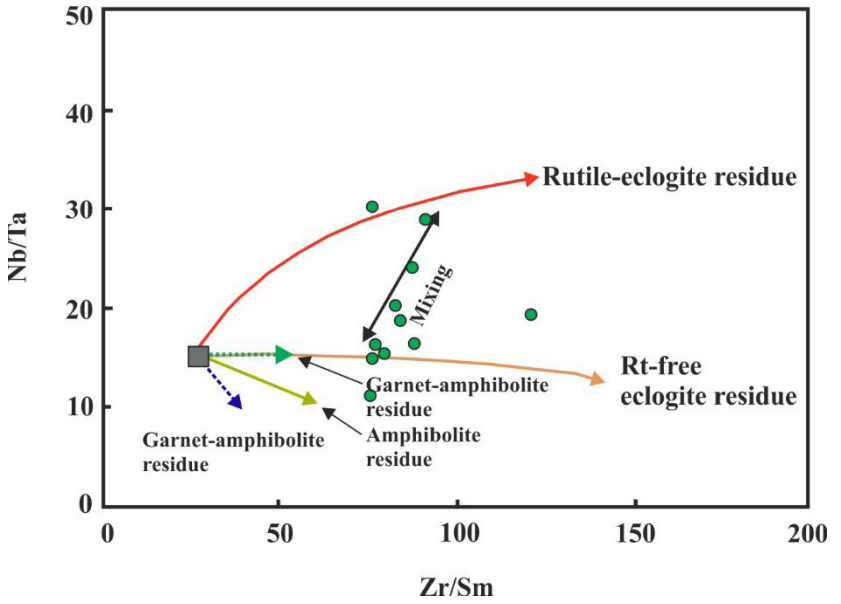

Figure 9. Zr/Sm versus Nb/Ta magma source composition discriminating plot for the trondhjemites from Tasiast terrain [Hoffmann et al., 2011]. Amphibole/melt partition coefficients of Foley [2008] (blue arrow); amphibole/melt partition coefficients of Klein et al. (1997) (green arrow).

and cannot be used for discriminating its tectonic settings.

In addition, the Tasiast unit occurs as Archean continental crust and is dominated by grey gneiss complexes (mainly trondhjemites, dated at about ~3.07–2.91 Ga [Chardon, 1997, Heron et al., 2016, Key et al., 2008]. Hence, the emplacement of these rocks is envisaged to represent the growth of new continental crust by partial melting of mantle that generate oceanic tholeiites (now amphibolites and eclogites), followed by the partial melting of these metabasalts to constitute the parental magma of studied Tasiast trondhjemitic gneisses. On the other hand, the Tasiast granitic gneisses are produced afterwards by partial melting of trondhjemitic gneisses (see Section 6.2). The age of granitization is unknown but it seems to be younger than 2.91 Ga and can be linked to an early stage of new crustal growth in the West African craton. These granites should be probably similar to the syn-tectonic high-K granites of the Tiris complex (Mauritania) that yielded an age of about 2.56–2.48 Ga [Schofield et al., 2012]. This comparison is strengthened by the recognition in Tasiast terrains of an important thermal imprint at that time [Chardon, 1997, Key et al., 2008].

7. Conclusion

Field and petrographic observations, and geochemistry data from the Tasiast Archean unit presented in this study allowed to formulating the following conclusions:

(1) Tasiast area consists mainly of trondhjemitic gneisses which host the high-K granites.

(2) Geochemical composition of the Tasiast trondhjemites suggests that they are juvenile continental crust generated by polybaric melting of metabasalts occurred over a range of P–T conditions, covering the stability fields of garnet amphibolite and rutile eclogite, and the melt has occurred without any mantle wedge involvement.

(3) Field relationships and trace element composition provide a genetic link between the trondhjemite and the high-K granitic gneisses.

(4) Our new field and petrographic observations, and geochemical data highlight at least two stages of magmatic events in the Tasiast Archean unit as follows: (1) a trondhjemite gneiss which is the earliest known gneiss in the region; (2) high-K granite which was generated by a partial melting of trondhjemites.

Acknowledgements

This paper is a contribution part of the PhD project of M. Bouha funded and supported by the FP7-PEOPLE-2013-IRSES project MEDYNA: Maghreb-Eu research staff exchange on geodynamics, geohazards, and applied geology in Northwest Africa 2014–2017, WP3–Deep structures and mantle processes. We would like to thank Carlos J. Garrido, co-coordinator of MEDYNA, for using the analytical facilities of Petrology, Geochemistry, and Geochronology department (PGG), IACT-CSIC, Granada. We also thank all the PGG members for their help in sample preparation and assistance in laboratory work. We would like to thank François Chabaux for editorial handling, and reviewers for their corrections and constructive remarks.

References

Arndt, N. T. (2013). The formation and evolution of the continental crust. *Geochem. Perspect.*, 2(3), 405–405.

Barker, F. (1979). Trondhjemites: definition, environment and hypotheses of origin. In Barker, F., editor, *Trondhjemites, Dacites and Related Rocks*, pages 1–12. Elsevier, Amsterdam.

Barker, F. and Arth, J. G. (1976). Generation of trondhjemitic–tonalitic liquids and Archean bimodal trondhjemite–basalt suites. *Geology*, 4, 596–600.

Beard, J. S. and Lofgren, G. E. (1989). Effect of water on the composition of partial melts of greenstones and amphibolites. *Science*, 244, 195–197.

Beard, J. S. and Lofgren, G. E. (1991). Dehydration melting and water saturated melting of basaltic and andesitic greenstones and amphibolites at 1, 3 and 6.9 kb. *J. Petrol.*, 32, 465–501.

Bessoles, B. (1977). *Géologie de l'Afrique : le craton ouest-africain*. Mem. BRGM, Paris.

Cahen, L., Snelling, N. J., Delhal, J., Vail, J. R., Bonhomme, M., and Ledent, D. (1984). *The Geochronology and Evolution of Africa*. Oxford University Press, Oxford. Royaume-Uni.

Chardon, D. (1997). *Les déformations continentales Archéennes. Exemples naturels et modélisation thermomécanique*. Mémoires de Géosciences. Rennes.

Chorlton, L. B. (2007). Generalized geology of the world: bedrock domains and major faults in GIS 416 format: a small scale world geology map with an extended geological attribute database. *Geol. Surv. Canada*, 5529, 48.

Condie, K. C. (1989). *Plate Tectonics and Crustal Evolution*. Pergamon Press, Oxford.

Condie, K. C. (1993). Chemical composition and evolution of the upper continental crust; contrasting results from surface samples and shales. *Chem. Geol.*, 104, 1–37.

Condie, K. C. (2005). TTGs and adakites: are they both slab melts? *Lithosphere*, 79, 33–44.

Davidson, J., Macpherson, C., and Turner, S. (2007). Amphibole control in the differentiation of arc magmas. *Geochim. Cosmochim. Acta*, 71, article no. A204.

De Almeida, J. A. C., Dall'agnol, R., and Rocha, M. C. (2017). Tonalite–trondhjemite and leucogranodiorite–granite suites from the Rio Maria domain, Carajás Province, Brazil: implications for discrimination and origin of the Archean Na-granitoids. *Canad. Mineral.*, 55(3), 437–456.

Dey, S., Topno, A., Liu, Y., and Zong, K. (2017). Generation and evolution of Palaeoarchaean continental crust in the central part of the Singhbhum craton, eastern India. *Precamb. Res.*, 298, 268–291.

Dillon, W. P. and Sougy, J. M. A. (1974). Geology of West Africa and Canary and Cape Verde islands. In Nairn, A. E. M. and Stehl, F. G., editors, *The Ocean Basins and Margins*, volume 2, pages 315–390. The North Atlantic. Plenum, New York.

Drummond, M. S. and Defant, M. J. (1990). A model for trondhjemite–tonalite–dacite genesis and crustal growth via slab melting: Archean to modern comparisons. *J. Geophys. Res.*, 95, 21503–21521.

Ennih, N. and Liégeois, J. P., editors (2008). *The Boundaries of the West African Craton*, volume 297 of *Special Publications*. Geological Society, London.

Foley, S. (2008). A trace element perspective on Archean crust formation and on the presence or absence of Archean subduction. *Geol. Soc. Am., Sp. Papers*, 440, 31–50.

Foley, S., Tiepolo, M., and Vannucci, R. (2002). Growth of early continental crust controlled by melting of amphibolite in subduction zones. *Nature*, 417, 837–840.

Garrido, C. J., Bodinier, J. L., and Alard, O. (2000). Incompatible trace element partitioning and res-

idence in anhydrous spinel peridotites and websterites from the Ronda orogenicperidotite. *Earth Planet. Sci. Lett.*, 181, 341–358.

Hamilton, W. B. (1998). Archean magmatism and deformation are not products of plate tectonics. *Precamb. Res.*, 91, 145–179.

Hamilton, W. B. (2003). An alternative earth. *GSA Today*, 13(11), 4–12.

Helz, T. (1976). Phase relations in basalts in their melting range at P(H_2O) = 5 kb. Part II: melt compositions. *J. Petrol.*, 17, 139–193.

Heron, K., Jessell, M., Benn, K., Harris, E., and Quentin Crowley, Q. G. (2016). The Tasiast deposit, Mauritania. *Ore Geol. Rev.*, 78, 564–572.

Hoffmann, J. E., Münker, C., Næraa, T., Garbe-Schönberg, D., and Svahnberg, H. (2011). Mechanisms of Archean crust formation inferred from high-precision HFSE systematics in TTGs? *Geochim. Cosmochim. Acta*, 75, 4157–4178.

Hoffmann, J. E., Nagel, T. J., Münker, C., Næraa, T., Minik, T., and Rosing, M. T. (2014). Constraining the process of Eoarchean TTG formation in the Itsaq Gneiss Complex, southern West Greenland. *Earth Planet. Sci. Lett.*, 388, 374–386.

Holloway, J. R. and Burnham, C. W. (1972). Melting relations of basalt with equilibrium water pressure less than total pressure. *J. Petrol.*, 13, 1–29.

Huang, H., Polat, A., and Fryer, B. J. (2013). Origin of Archean tonalite–trondhjemite–granodiorite (TTG) suites and granites in the Fiskenæsset region, southern West Greenland: implications for continental growth. *Gondwana Res.*, 23, 452–470.

Jahn, B. (1994). Géochimie des granitoïdes archéens de la croute primitive. In Hagemann, R., Jouzel, J., Treuil, M., and Turpin, L., editors, *La géochimie de la Terre*. CERA, Masson, Paris.

Jahn, B. M., Glikson, A. Y., Peucat, J. J., and Hickman, A. H. (1981). REE geochemistry and isotopic data of Archaean silica volcanics and granitoids from the Pilbara Block, western Australia: implications for the early crustal evolution. *Geochim. Cosmochim. Acta*, 45, 1633–1652.

Jenner, G. A., Foley, S. F., Jackson, S. E., Green, B. J., Fryer, H. P., and Long Erich, H. P. (1994). Determination of partition coefficients for trace elements in high pressure–temperature run products by laser ablation microprobe-inductively coupled plasma mass spectrometry (LAM-ICP-MS). *Geochim. Cosmochim. Acta*, 58, 5099–5103.

Jochum, K. P., Weis, U., Schwager, B., Stoll, B., Wilson, S. A., Haug, G. H., Andreae, M. O., and Enzweiler, J. (2016). Reference values following ISO guidelines for frequently requested rock reference materials. *Geostandards Geoanal. Res.*, 40, 333–350.

Key, R. M., Loughlin, S. C., Horstwood, M. S. A., Gillespie, M., Pitfield, P. E. J., Henney, P. J., Crowley, Q. G., and Del Rio, M. (2008). Two Mesoarcheanterranes in the Reguibat shield of NW Mauritania. In Ennih, N. and Liégeois, J. P., editors, *Boundaries of the West African Craton*, volume 297 of *Special Publications*, pages 33–52. Geological Society, London.

Klemme, S., Blundy, J. D., and Wood, B. J. (2002). Experimental constraints on major and trace element partitioning during partial melting of eclogite. *Geochim. Cosmochim. Acta*, 66, 3109–3123.

Klemme, S., Prowatke, S., Hametner, K., and Günther, D. (2005). Partitioning of trace elements between rutile and silicate melts: implications for subduction zones. *Geochim. Cosmochim. Acta*, 49, 2361–2371.

Laurent, O., Martin, H., Moyen, J. F., and Doucelance, R. (2014). The diversity and evolution of Late-Archeangranitoids: evidence for the onset of "modern-style" plate tectonics between 3.0 and 2.5 Ga. *Lithos*, 205, 208–235.

Macpherson, C. G., Dreher, S. T., and Thirlwall, M. F. (2006). Adakites without slab melting: high pressure processing of basaltic island arc magma, Mindanao, the Philippines. *Earth Planet. Sci. Lett.*, 243, 581–593.

Maniar, P. D. and Piccoli, P. M. (1989). Tectonic discrimination of granitoids. *Geol. Soc. Am. Bull.*, 101, 635–643.

Martin, H. (1994). The Archean grey gneisses and the genesis of continental crust. In Condie, K. C., editor, *The Archean Crustal Evolution*, Developments in Precambrian Geology, pages 205–259. Elsevier, Amsterdam.

Martin, H. (1999). Adakitic magmas: modern analogues of Archaean granitoids. *Lithos*, 46, 411–429.

Martin, H. and Moyen, J. F. (2002). Secular changes in TTG composition as markers of the progressive cooling of the Earth. *Geology*, 30, 319–322.

Martin, H., Moyen, J. F., Guitreau, M., Blichert-Toft, J., and Le Pennec, J. L. (2014). Why Archaean TTG cannot be generated by MORB melting in subduction zones. *Lithos*, 198, 1–13.

Martin, H., Smithies, R. H., Rapp, R., Moyen, J. F.,

and Champion, D. (2005). An overview of adakite, tonalite–trondhjemite–granodiorite (TTG), and sanukitoid: relationships and some implications for crustal evolution. *Lithos*, 79, 1–24.

McDonough, W. F. and Sun, S. S. (1995). The composition of the Earth. *Chem. Geol.*, 120, 223–253.

Menchikoff, N. (1949). Quelques traits de l'histoire géologique du Sahara occidental. Livre jubilaire Charles Jacob. *Ann. Hêbat et Haug*, 7, 303–325.

Montero, P., Haissen, F., Archi, A. E., Rjimati, E., and Bea, F. (2014). Timing of Archean crust formation and cratonisation in the Awsard-Tichla zone of the NW Reguibat Rise, West African Craton. A SHRIMP, Nd–Sr isotopes, and geochemical reconnaissance study. *Precamb. Res.*, 242, 112–137.

Moyen, J. F. (2009). High Sr/Y and La/Yb ratios: the meaning of adakiticsig, nature. *Lithos*, 112, 556–574.

Moyen, J. F. (2011). The composite Archaean grey gneisses: petrological significance, and evidence for a non-unique tectonic setting for Archaean crustal growth. *Lithos*, 123, 21–36.

Moyen, J. F., Laurent, O., Chelle-Michou, C., Couzini'e, S., Vanderhaeghe, O., Zeh, A., Villaros, A., and Gardien, V. (2017). Collision versus subduction-related magmatism: two contrasting ways of granite formation and implications for crustal growth. *Lithos*, 277, 154–177.

Moyen, J. F. and Martin, H. (2012). Forty years of TTG research. *Lithos*, 148, 312–336.

O'Connor, J. T. (1965). A classification for quartz-rich igneous rocks based on feldspar ratios. *U.S. Geol. Surv. Res.*, 0525-B, B79–B84.

O'Neil, J. and Carlson, R. W. (2017). Building Archean cratons from Hadean mafic crust. *Science*, 355, 1199–1202.

Ouabid, M., Ouali, H., Garrido, C. J., Acosta-Vigil, A., Román-Alpiste, M. J., Dautria, J. M., Marchesi, C., and Hidas, K. (2017). Neoproterozoic granitoids in the basement of the Moroccan Central Meseta: correlation with the Anti-Atlas at the NW paleomargin of Gondwana. *Precamb. Res.*, 299, 34–57.

Patino Douce, A. E. (2005). Vapor-absent melting of tonalite at 15–32 kbar. *J. Petrol.*, 46, 275–290.

Peccerillo, R. and Taylor, S. R. (1976). Geochemistry of Eocene calc-alkaline volcanic rocks from the Kastamonu areas, northern Turkey. *Contrib. Mineral. Petrol.*, 58, 63–81.

Rapp, K. P., Shimizu, N., and Norman, M. (2003). Growth of early continental crust by partial melting of eclogite. *Nature*, 425, 605–609.

Rapp, R. P., Shimizu, N., Norman, M. D., and Applegate, G. S. (1999). Reaction between slabs derived melts and perioite in the mantle wedge. Experimental constraints at 3.8 GPa. *Chem. Geol.*, 160, 335–356.

Rapp, R. P. and Watson, E. B. (1995). Dehydration melting of metabasalt at 8–32 kbar: implications for continental growth and crust mantle recycling. *J. Petrol.*, 36, 891–931.

Rubatto, D. and Hermann, J. (2003). Zircon formation during fluid circulation in eclogites (Monviso, western Alps); implications for Zr and Hf budget in subduction zones. *Geochim. Cosmochim. Acta*, 67, 2173–2187.

Rudnick, R. L. (1995). Making continental crust. *Nature*, 378, 571–578.

Rushmer, T. (1991). Partial melting of two amphibolites: contrasting experimental results under fluid-absent conditions. *Contrib. Mineral. Petrol.*, 107, 41–59.

Schofield, D., Horstwood, M. S. A., Pitfield, P. E. J., Crowley, Q. G., Wilkinson, A. F., and Sidat, H. C. O. (2006). *J. Geol. Soc. Lond.*, 163, 549–560.

Schofield, D. I., Horstwood, M. S. A., Pitfield, P. E. J., Gillespie, M., Darbyshire, F., O'Connor, E. A., and Abdouloye, T. B. (2012). U–Pb dating and Sm–Nd isotopic analysis of granitic rocks from the Tiris complex: new constaints on key events in the evolution of the Reguibat Shield, Mauritania. *Precamb. Res.*, 204/205, 1–11.

Sen, C. and Dunn, T. (1994). Dehydration melting of a basaltic composition amphibolite at 1.5 and 2.0 GPa: implications for the origin of adakites. *Contrib. Mineral. Petrol.*, 117, 394–409.

Smithies, R. H. (2000). The Archaean tonalite–trondhjemite–granodiorite (TTG) series is not an analogue of Cenozoic adakite. *Earth Planet. Sci. Lett.*, 182, 115–125.

Smithies, R. H. and Champion, D. C. (1998). High-Mg diorite from the Archaean Pilbara Craton: anorogenic magmas derived from a subduction-modified mantle. *Geol. Surv. West. Australia Ann. Rev.*, 1999, 45–59.

Smithies, R. H., Lu, Y., Johnson, T. E., Kirkland, C. L., Cassidy, K. F., Champion, D. C., and Poujol, M. (2019). No evidence for high-pressure melting of Earth's crust in the Archean. *Nature*, 10, 1–12.

Sun, S. S. and McDonough, W. F. (1989). Chemical and isotopic systematics of oceanic basalts: implications for mantle composition and processes. In Saunders, S. D. and Norry, M. J., editors, *Magmatism in Ocean Basins*, volume 42, pages 313–345. Geological Society, London.

Tarney, J., Weaver, B. L., and Winley, B. F. (1982). Geological and geochemical evolution of the Archaean continental crust. *Rev. Bras. Geoci.*, 12, 53–59.

Van Kranendonk, M. J., Hickman, A. H., Smithies, R. H., and Champion, D. C. (2007). Paleoarchean development of a continental nucleus: the East Pilbara terrane of the Pilbara craton, Western Australia. In Van Kranendonk, M. J., Smithies, R. H., and Bennet, V., editors, *Earth's Oldest Rocks*, Developments in Precambrian Geology, pages 307–337. Elsevier.

Watkins, J., Clemens, J., and Treloar, P. (2007). Archaean TTGs as sources of younger granitic magmas: melting of sodic meta-tonalites at 0.6–1.2 GPa. *Contrib. Mineral. Petrol.*, 154, 91–110.

Winther, K. T. and Newton, R. C. (1991). Experimental melting of hydrous low-K tholeiite: evidence on the origin of Archaean cratons. *Bull. Geol. Soc. Denmark*, 39, 213–228.

Wu, F. Y., Jahn, B. M., Wilde, S. A., Lo, C. H., Yui, T. F., Lin, Q., Ge, W. C., and Sun, D. Y. (2003). Highly fractionated I-type granites in NE China (I): geochronology and petrogenesis. *Lithos*, 66, 241–273.

Xiong, X. L. (2006). Trace element evidence for growth of early continental crust by melting of rutile-bearing hydrous eclogite. *Geology*, 34, 945–948.

Xiong, X. L., Han, J. W., and Wu, J. H. (2007). Phase equilibrium and trace element partitioning between minerals and melt in the metabasalt system: constraints on the formation conditions of TTG/adakite magmas and the growth of early continental crust. *Earth Sci. Frontiers*, 14, 151–158.

Zhai, M. G. and Santosh, M. (2011). The early Precambrian odyssey of the North China Craton: a synoptic overview. *Gondwana Res.*, 20, 6–25.

Zhou, Y., Zhao, T., Zhai, M., Gao, J., and Sun, Q. (2014). Petrogenesis of the Archean tonalite–trondhjemite–granodiorite (TTG) and granites in the Lushan area, southern margin of the North China Craton: implications for crustal accretion and transformation. *Precamb. Res.*, 255, 514–537.